

A Simulation of the Enthalpies of Fusion of Unplasticized Poly(vinyl Chloride)

O. P. OBANDE

Department of Chemistry, Ahmadu Bello University, Zaria, Nigeria

SYNOPSIS

Enthalpies of fusion were measured by differential scanning calorimetry for PVC compounds processed within the range 150°–220°C by twin-screw extrusion or compression molding. It was observed that the effects of polymer molar mass (*K*-value) or sample formulation on values of the experimental enthalpy change follow identical pattern as effects of the same parameter on elastic response established by rheometry. It was assumed that the “amorphous” phase is made up of a matrix of locally ordered chain segments and occluded free-volume and that this matrix constitutes what is described as “secondary crystallinity” of bulk PVC. On the basis of this assumption, a model was developed incorporating a parameter for the contribution of enthalpy of relaxation of free volume to the observed enthalpy of fusion of the secondary crystallinity. Graphical comparison of the simulated enthalpy changes with the measured values produced accurate measures of the critical temperature where a change in melt flow activation energy has been established by rheometry. The comparison further predicts that if PVC was processed below 190°C, an increase in shear intensity should reduce the free-volume content of the product, while processing above 200°C should result in the converse. Also, with increasing processing temperature above 200°C a shear-independent linear decrease in free-volume of the bulk product is suggested to be operative. Thus, the material produced by extrusion or compression molding between 190 and 200°C should be least dense and least crystalline in line with previous observations.

INTRODUCTION

Differential scanning calorimetry (DSC) of unplasticized PVC shows several regions of endothermal activity; some of these are illustrated in Figure 1. Depending on the rates of heating and cooling, an endothermal peak *S* is superimposed on the glass transition, T_g , baseline shift. Where samples have been suddenly quenched during processing, an endotherm *R* occurs below T_g . Illers¹ has shown that the endotherms *R* and *S* give a measure of the enthalpy of relaxation arising as a result of reduction in the concentration of vacant spaces within the amorphous phase during annealing below T_g .

Most of the (primary) crystals in commercial grade PVC melt² in the range 100–230°C. The virgin polymer gives a single endotherm in this region

whereas the processed material gives two endotherms as shown in Figure 1. According to Illers,² the wide melting range arises as a result of distribution of crystal size and crystal perfection. This is normally expected for semicrystalline polymers³ except that the range for PVC is unusually wide. According to Juijn et al.,⁴ during processing melted primary crystals of the resin powder recrystallize on cooling to give a defective ordered state described as secondary crystallinity. In subsequent calorimetry of the processed sample fusion of the secondary crystallinity produces an endotherm, *A*, in the lower temperature region while fusion of primary crystals, annealed during processing, produces the higher temperature endotherm, *B*, shown in Figure 1. The onset temperature of the endotherm *B*, T_B , measures the temperature at which the unmelted primary crystals were annealed.^{2,5} In effect it gives an accurate measure of the maximum temperature of the melt during processing.⁶

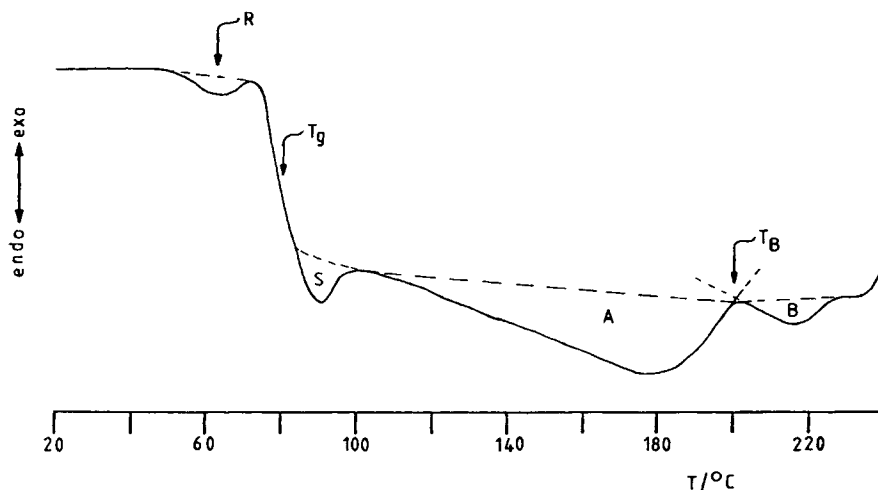


Figure 1 DSC trace of PVC (sample L66A) extruded at 200°C.

If, as has been suggested,^{2,7} PVC crystalline fusion could be quantified by calorimetry using the endotherm A, this would increase the material quality control options. First, however, we need to understand properly the factors contributing to the size of the relevant endotherm. The enthalpy of fusion measured for a given crystal population normally depends on a number of factors, including fraction of repeat units in the crystalline phase, crystal perfection, size of crystal, and vacant spaces or "free-volume" occluded in the crystal.⁸ Some of these factors, of course, also depend on cooling rate from the melt and annealing conditions before calorimetry. Based on a distribution of ordered structures and taking into account enthalpy change due to relaxation of free-volume entrapped in the crystalline phase, it is possible to simulate the enthalpy of fusion of processed PVC. The procedure is presented.

MODEL

We assume that commercial PVC homopolymer is a random copolymer consisting of N_c units which crystallize and N_n units which do not, according to Flory depression of the melting point of the former by the latter, is described by the expression

$$1/T_m - 1/T_m^0 = -(R/\Delta H_u) \ln N_c \quad (1)$$

where T_m = melting point of the imperfect (secondary) crystal, T_m^0 = equilibrium melting point of the perfectly crystalline PVC, R = gas constant, and ΔH_u = enthalpy of fusion of the perfect PVC crystal.

Given a distribution of ordered units in bulk PVC, the enthalpy change, $\Delta H(T)_{\text{obs}}$, measured for the

material processed at a temperature T will be the average value of all enthalpy changes ΔH_i contributing to the total quantity $N_f(T)$ of units fused and recrystallized during processing. This is a weighted average since those factors which contribute most to the total units $N_f(T)$ fused will contribute most to the enthalpy change $\Delta H(T)_{\text{obs}}$, that is,

$$\Delta H(T)_{\text{obs}} = \sum_i g_i \frac{N_{fi}}{N_f(T)} \Delta H_i \quad (2)$$

where $N_f(T) = \sum N_{fi}$, N_{fi} being the number of repeat units in the i th secondary crystal population, the general term $N_{fi}/N_f(T)$ represents the contribution of the i th process having the enthalpy change ΔH_i , and the function g_i accounts for contributions from enthalpy of relaxation of occluded free-volume or defect concentration. Replacing N_c by N_{fi} in eq. (1), we get

$$N_{fi} = \exp\{-[\Delta H_i/R(1/T_i - 1/T_m^0)]\} \quad (3)$$

where T_m^0 is the equilibrium melt temperature of the perfect PVC crystal. From a critical survey of the literature the value $T_m^0 = 538$ K reported by Gouinlock⁹ was used in this study. Substitutions for $N_f(T)$ and N_{fi} in eq. (2) give

$$\begin{aligned} \Delta H(T)_{\text{obs}} &= \frac{\sum_i g_i \Delta H_i \exp\{-[\Delta H_i/R(1/T_i - 1/T_m^0)]\}}{\sum_i \sum_j \exp\{-[\Delta H_i/R(1/T_i - 1/T_m^0)]\}} \quad (4) \end{aligned}$$

The function g_i can be separated into two components, one of which depends on stiffness of the chain molecule and is, therefore, constant and the other of which depends on processing temperature. During processing creation of a defective structure in the form of vacant space within the crystalline phase would necessitate elastic deformation and freezing of the segment of the chain molecule forming the boundary of the space. As a result, g_i should depend linearly on processing temperature, that is,

$$g_i = a + bT_i \quad (5)$$

where a takes account of chain stiffness and b is the temperature coefficient. At the moment we are only able to evaluate a and b empirically; the procedure is described in due course.

EXPERIMENTAL

Sample Preparation

Suspension "Corvic" (ICI) and "Breon" (BP Chemicals) PVC homopolymers were used. The range of formulations is shown in Table I. Dry blends were prepared in an 8-L Fielder high speed mixer. They were then extruded or compression molded at temperatures of 150–220°C in approximately 10°C steps.

Two "Breon" compounds (L66A and L66B), K -value 66, containing unequal levels of the lubricant system were extruded with a Leistritz LS-30 : 34

twin-screw extruder fitted with 3 × 20 mm strip die and operated at 20 rpm. "Corvic" PVC, K -values 57, 62, 67, and 71 (KM57–KM71), containing equal additive levels were extruded using a Krauss Maffei KMDL-25 twin-screw extruder fitted with 4 × 30 mm strip die and operated at 20 rpm. The use of the two extruders under apparently similar conditions produced differences in sample shear history, the Leistritz samples having undergone the more severe shear history.

The "Breon" PVC was also formulated with levels of the lubricant system ranging from 0 to 7.5 phr as shown in Table I (CM661–CM667). The dry blends were pressed at 70 bar to produce fused sheets of size 4 × 200 mm. High lubricant levels were used so that effective zero shear conditions could be investigated.

Calorimetry

Measurements were made with a DuPont 990 analyzer equipped with a differential scanning calorimetry (DSC) cell. A 10-mg sample was heated from room temperature to 240°C at 20°C/min. A typical trace is illustrated in Figure 1. Traces for similar samples showing the effect of increasing processing temperature have been reported.^{2,5,6} Values of $\Delta H(T)_{\text{obs}}$ were calculated from the area of the endotherm A using indium as standard material and the expression

$$\Delta H(T)_{\text{obs}} = KA/W \quad (6)$$

Table I Compound Formulations in Parts by Weight

Sample Code	PVC	Dibasic Lead Stearate	Stanclere T135 ^a	Normal Lead Stearate	Calcium Stearate	Wax ^b GS2411P
L66A	100 ^c	2.5	—	—	0.8	0.3
L66B	100 ^c	1.5	—	1.5	0.4	0.3
KM57	100 ^d	—	3.0	—	0.8	0.3
KM62	100 ^d	—	3.0	—	0.8	0.3
KM68	100 ^d	—	3.0	—	0.8	0.3
KM71	100 ^d	—	3.0	—	0.8	0.3
CM661	100 ^c	—	3.0	—	—	—
CM662	100 ^c	—	3.0	—	3.0	0.25
CM663	100 ^c	—	3.0	—	3.0	0.5
CH664	100 ^c	—	3.0	—	3.0	1.0
CM665	100 ^c	—	3.0	—	3.0	1.5
CM666	100 ^c	—	3.0	—	3.0	3.0
CM667	100 ^c	—	3.0	—	3.0	4.5

^a Supplied by Akzo Chemie.

^b Supplied by Cornelius Co.

^c Breon S110/11, K -value 66.

^d Corvic PVC homopolymers with K values as sample code.

where W = sample mass, A = peak area, and K = const related to instrument setting.

Testing the Model

Equation (4) can be solved only by curve fitting either numerically or graphically. The numerical method is lengthy and without the benefit of improved results; therefore, a graphical method is used. To simplify computation, we start by assuming that g_i is independent of temperature and therefore constant, i.e., $g_i = 1.0$. Equation (4) then reduces to

$$\Delta H(T)_{\text{obs}} = \frac{\sum_i \Delta H_i \exp\{-[\Delta H_i/R(1/T_i - 1/T_m^0)]\}}{\sum_i \sum_j \exp\{-[\Delta H_i/R(1/T_i - 1/T_m^0)]\}} \quad (7)$$

Equation (7) is solved graphically as follows: Representative values of ΔH_i are extracted at $T_i = 1^\circ\text{C}$ intervals from plots of $\Delta H(T)_{\text{obs}}$ vs. T corrected for scatter as shown in Figures 2 and 3. The values are substituted in eq. (7) and "theoretical" values of the enthalpy change, $\Delta H(T)_{\text{calcd}}$, computed with the

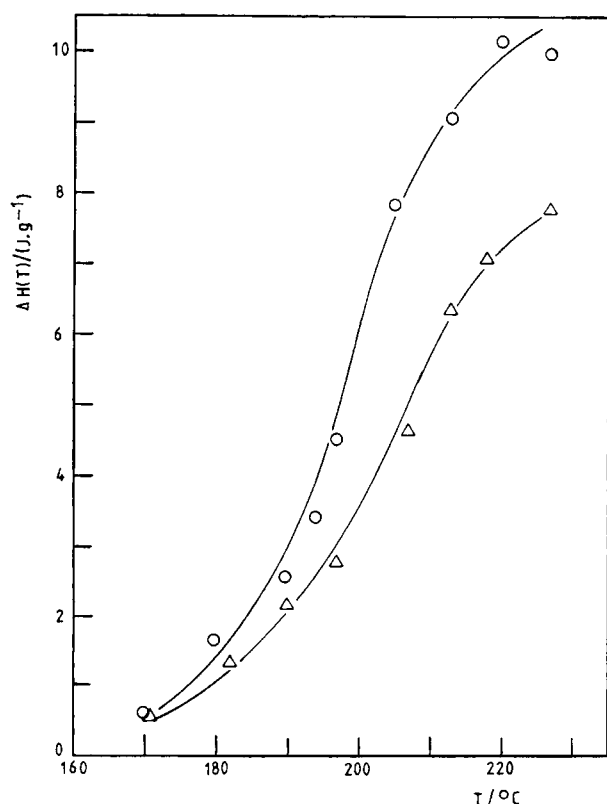


Figure 2 Change of heat of fusion with processing temperature for samples: (○) L66A; (△) L66B.

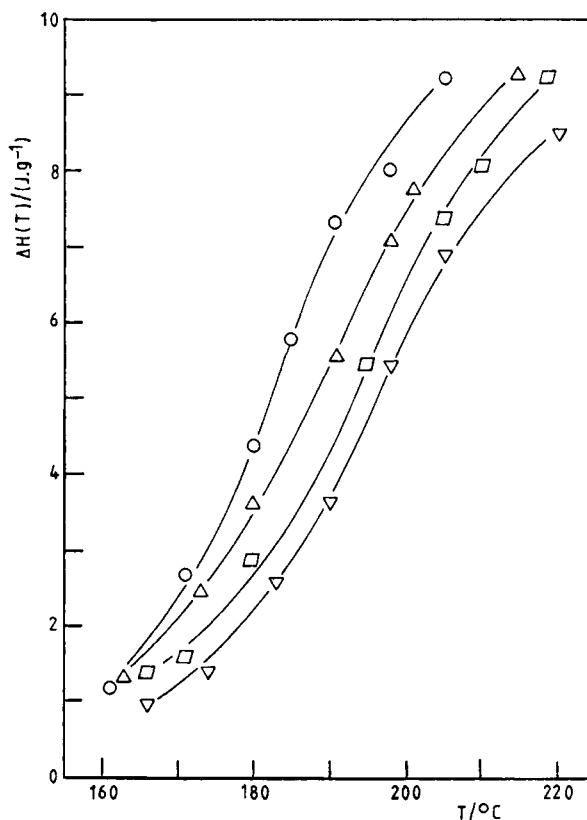


Figure 3 Change of heat of fusion with processing temperature for samples: (○) KM57; (△) KM62; (□) KM67; (▽) KM71.

aid of a simple programme. A result of this procedure is presented in Figure 4 for sample L66A. The two curves have the same shape, but the calculated curve progressively falls short of the experimental with increase in processing temperature. From Figure 4, we observed a difference of 5 J/g between the predicted and measured enthalpy change at the limit of the experimental processing temperature. The value is higher than the value 2.5 J/g obtained from annealing by Illers^{1,2} for the excess enthalpy in the glassy state. The difference is thought to be caused by the effects of shear on the defect concentration. Normally, recrystallization from the melt would be more defective with increased melt shear intensity. Accordingly, the relative values of the observed and predicted enthalpy change would depend on the process shear regime.

It turns out that the ratio $\Delta H(T)_{\text{obs}}/\Delta H(T)_{\text{calcd}}$ calculated from Figure 4 is linear over the processing temperature range studied. At the moment, this ratio is significant only to the extent that it evaluates the amount by which the value of the experimental enthalpy exceeds the calculated approximate value.

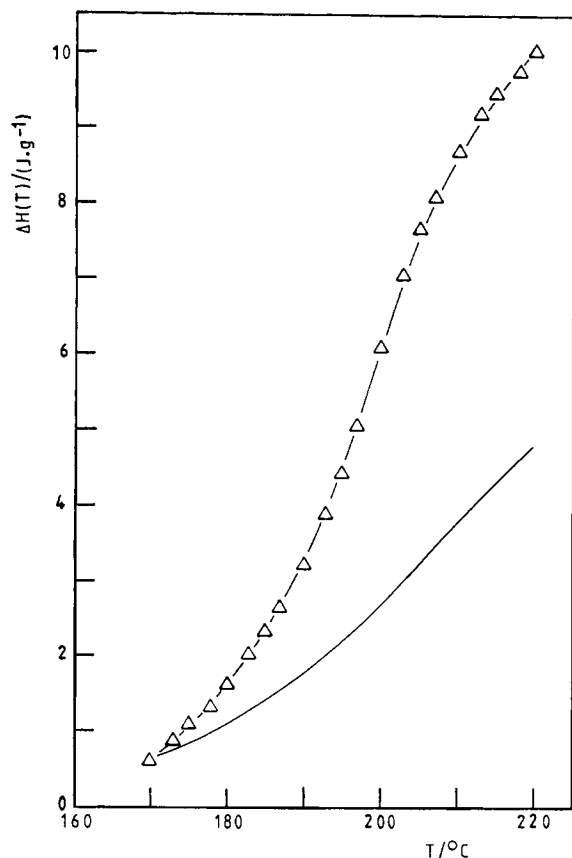


Figure 4 Comparison of eq. (7) with experimental results based on sample L66A; (Δ) experimental; (—) calculated.

The limits of the ratio of the two quantities at the starting and final processing temperatures are approximately 1.0 and 2.0. Substituting these values for g_i in eq. (5) and solving the resultant simultaneous equations using the respective temperature limits 433 and 503 K gives $a = -5.18$ and $b = 1.43 \times 10^{-2}$. The value of b suggests that the defect concentration of the secondary crystalline phase increases by 1.43% with a degree rise of processing temperature. The negative value of a is consistent with the fact that chain stiffness reduces the chances of creating a vacancy within the crystal structure. Substituting the values of a and b in eq. (4) and solving the resultant expression as described above gives a set of values of $\Delta H(T)_{\text{calcd}}$, which compares well with experimental values.

RESULTS AND DISCUSSION

We consider first values of the experimental enthalpies. The subject has been studied at length by

Gilbert,⁷ here we provide additional information on the effects of polymer K value and lubricant concentration. The effect of the latter on variation of $\Delta H(T)_{\text{obs}}$ with processing temperature is illustrated in Figure 2 for the extrudates L66A and L66B. Similar effects are presented in Table II for the molded samples. For the extrudates the fusion level corresponding to $\Delta H(T)_{\text{obs}} = 3.5$ J/g occurs at processing temperatures of 190 and 200°C for total lubricant (calcium stearate + wax) levels of 1.1 and 2.2 phr, respectively, whereas for the molded sample (Table II) the $\Delta H(T)_{\text{obs}}$ value of the order of 5 J/g occurs at 186, 201, 210, and 220°C for total lubricant loadings of 0, 4.0, 6.0, and 7.5 phr, respectively. These results agree with results obtained from rheological measurements which have been reported by several authors and discussed at length by Krzewski and Collins.^{10,11} The rheological studies were concerned with development of the melt flow units. An increase in lubricant concentration was found to delay to higher temperatures breakdown of particulate units and interparticle network formation. The present results, showing a similar delay in crystalline fusion, suggest a strong link between the network and the secondary crystallinity of melt processed PVC.

The effect of the polymer K value is illustrated in Figure 3. At constant processing temperature the value of the enthalpy change is reduced as the polymer K -value, that is, molar mass, increases. In effect, equivalent crystalline fusion levels are shifted to higher processing temperatures with increasing molar mass of the resin. Similar results showing delay of network formation to higher processing temperatures with increase in molar mass are well established by rheometry.¹¹

It is pertinent to note that discrete ordering of chains as a unique interpretation of endothermal response is not necessary when dealing with amorphous polymers. According to Sheldon and associates,¹²⁻¹⁴ broad peaks are characteristic of amorphous polymers in keeping with a concept of free-volume entrapment on the one hand and local chain ordering on the other. The present evidence would suggest that the secondary crystallinity of bulk PVC could be a matrix of entrapped free-volume and locally ordered segments of the chain molecule.

Results of simulation of values of the experimental enthalpy change are presented in Figures 5, 6, and 7. Clearly, the success of the model is due largely to the use of the function g_i , which accounts for contribution to the total enthalpy change from enthalpy of relaxation of free-volume entrapped in the secondary crystalline phase. Differences in the relative positions of the experimental and calculated

Table II Changes in Enthalpy of Fusion of Molded PVC

Samples													
CM661		CM662		CM663		CM664		CM665		CM666		CM667	
T (°C)	$\Delta H(T)$ (J/g)	T (°C)	$\Delta H(T)$ (J/g)	T (°C)	$\Delta H(T)$ (J/g)	T (°C)	$\Delta H(T)$ (J/g)	T (°C)	$\Delta H(T)$ (J/g)	T (°C)	$\Delta H(T)$ (J/g)	T (°C)	$\Delta H(T)$ (J/g)
151	1.16	166	0.56	160	0.35	158	0.73	160	0.39	158	—	162	1.55
171	1.12	178	1.74	169	1.69	169	1.54	171	1.39	172	1.29	170	1.12
182	4.77	183	3.01	183	2.90	178	2.70	179	2.16	180	2.08	179	1.64
186	5.09	190	4.19	190	3.37	190	3.15	191	2.98	190	2.71	192	2.70
198	6.93	200	6.60	199	5.87	201	5.37	200	4.87	199	4.41	201	3.67
208	8.76	210	7.75	210	7.06	210	6.42	212	5.85	210	5.34	209	4.08
220	9.87	220	—	221	8.79	221	7.83	220	7.08	221	6.55	220	5.14

curve in Figures 5, 6, and 7 can be visualized in the light of relative free-volume population of the samples. Notice that the absolute value of the enthalpy change is independent of process shear regime.

For the extrudates, L and KM samples, the cal-

culated curve crosses the experimental curve at a temperature which depends on sample formulation and on polymer K -value. Thus for the L samples (Fig. 5) the two curves intersect at 190 and 194°C for lubricant levels of 1.1 and 2.2 phr, respectively.

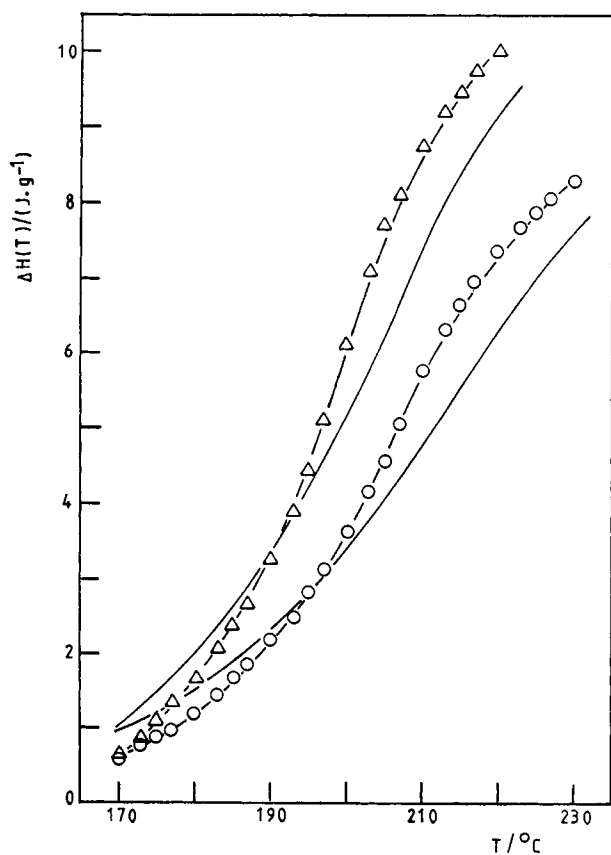


Figure 5 Comparison of calculated with experimental heats of fusion based on: (Δ) L66A; (\circ) L66B; (—) calculated.

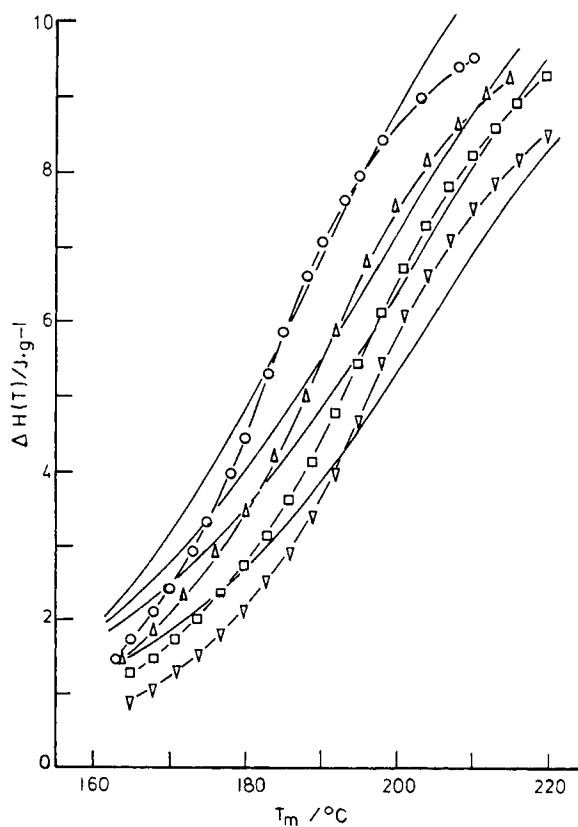


Figure 6 Comparison of calculated with experimental heats of fusion based on: (\circ) KM57; (Δ) KM62; (\square) KM67; (∇) KM71; (—) calculated.

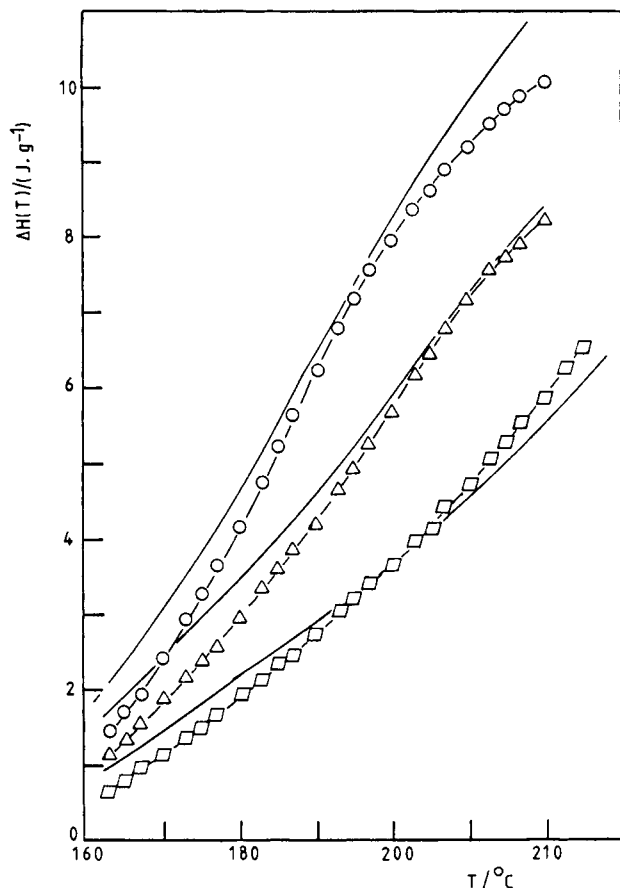


Figure 7 Comparison of calculated with experimental heats of fusion based on some CM samples: (O) CM661; (Δ) CM664; (\square) CM667; (—) calculated.

And for the KM samples (Fig. 6), the two curves intersect at 185, 192, 197, and 193°C for polymer K values 57, 62, 68, and 71, respectively. The discrepancy for K -71 polymer is thought to arise from major physical differences between this resin and others in the series. The K -71 polymer is a relatively high molar mass, $\bar{M}_w = 2.0 \times 10^5$, low density grade suitable for plasticization. For the KM samples (Fig. 6) a second intersection between the two curves may be observed at a higher temperature.

For the pressed sheets, Figure 7 shows that intersection of the calculated and experimental curve is dependent on the lubricant level. A tangential approach or intersection of the two curves occurs at 195, 210, and 200°C for lubricant levels of 0, 4.0, and 7.5 phr respectively.

The temperature at which the experimental and calculated curve approach tangentially or intersect, that is, where the calculated enthalpy change equals the experimental value, coincides in all cases with the critical temperature, T_{crit} , at which a change in

melt flow activation energy is known to occur.¹⁵ It is shown here that an increase in lubricant concentration or in polymer K -value shifts T_{crit} to higher values in exactly the same manner as found by rheometry.^{10,11,15}

Figures 5, 6, and 7 show that in all cases eq. (4) overestimates the experimental enthalpy change below T_{crit} ; in other words, contribution from enthalpy of relaxation of the entrapped free volume or indeed the free-volume population of the sample prepared below T_{crit} is lower than expected. Above T_{crit} , the relative position of the experimental and calculated curve depends on the processing history. If the sample is sufficiently sheared above T_{crit} , the experimental curve rises above the calculated curve, suggesting higher than predicted free-volume population of the processed sample as would be expected normally (Fig. 5). On the other hand, if with increasing processing temperature the melt viscosity does not permit sufficient shear the experimental curve falls again below the calculated curve, suggesting a fall in free-volume population below the predicted value. In this case the behavior illustrated in Figure 6 is perfectly in line with expectation. The melt viscosity at a given temperature will increase with an increase in the molar mass of the polymer. Accordingly, a second intersection of the two curves above T_{crit} is less likely with an increase in the polymer K -value.

Figure 7 shows that, over the processing temperature range studied, the enthalpy change obtained for the pressed sample falls below the predicted value. However, as lubricant concentration is increased, the two values approach closely at a given temperature. In other words, the free-volume population of the pressed sample is normally less than predicted but approaches the predicted value as lubricant concentration increases. It is, of course, expected that, with the absence of shear compression, molding should produce samples with reduced free-volume content. However, it is unexpected that an increase in lubricant concentration would give rise to values of enthalpy change which are closer to and in some cases higher than the predicted values, suggesting higher than predicted free-volume population. The lubricant melts below 100°C; therefore, it is not expected to contribute to the measured enthalpy change. We cannot explain this observation at the moment; an independent study is in progress to investigate the effects of lubricant concentration on the density of compression molded sheets.

Since the relative position of the experimental and calculated curve can be meaningfully interpreted in terms of free-volume population, it is obvious that

Table III $\Delta H(T)_{\text{obs}}/\Delta H(T)_{\text{calcd}}$ Values Calculated from Figures 5, 6, and 7

Sample	Melt Temperatures (°C)								
	170	175	180	185	190	195	200	210	220
L66A	0.55	0.67	0.78	0.89	1.0	1.01	1.17	1.14	1.10
KM67	0.64	0.71	0.78	0.85	0.92	0.96	1.03	1.01	0.98
CM661	0.80	0.85	0.90	0.93	0.87	0.97	0.96	0.94	0.91

values of the ratio $\Delta H(T)_{\text{obs}}/\Delta H(T)_{\text{calcd}}$ calculated from Figures 5, 6, and 7 for similarly formulated equivalent K -value polymers will reveal the effect of processing history on the free-volume population of the product. Samples L66A, KM67, and CM661 were selected from Figures 5, 6, and 7, respectively. The three samples were formulated using two polymer K -values 66 and 67 with $\bar{M}_w = 1.2 \times 10^5$ and 1.4×10^5 , respectively; details of formulation are provided in Table I. Values of the ratio of the enthalpy change calculated for the three samples are presented in Table III. Plots of the values against processing temperature reveal three regions of linearity as shown in Figure 8. Below 190°C the lines have positive slopes; the slope is steeper the more severe the shear history. Between 190 and 200°C there is a modest decrease in slope for the extrudate

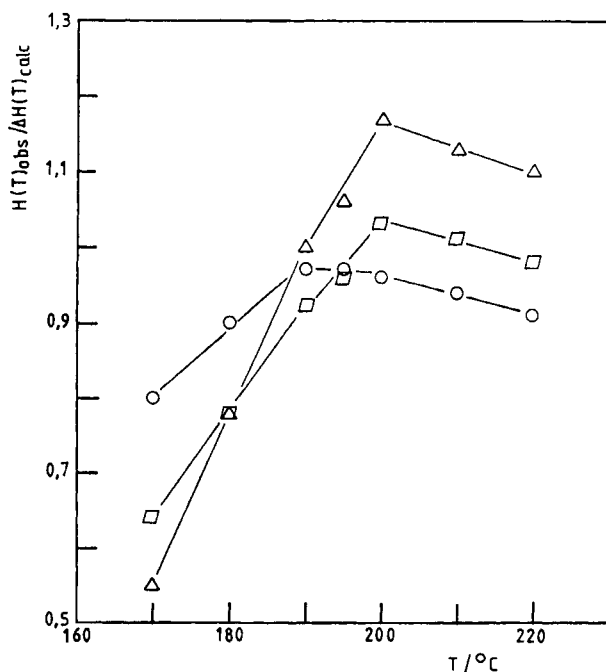


Figure 8 Plot of the ratio of observed to calculated heat of fusion for PVC samples: (Δ) L66A; (□) KM667; (○) CM661.

while a significant decrease is recorded for the compression molded sample. Above 200°C all the samples give lines with negative slopes, and, significantly, the value of the slope is constant and independent of shear history.

Figure 8 can be interpreted reasonably as illustrating the rate of change of free-volume population of the sample with increasing processing temperature. Thus, expectedly, the higher the process shear intensity the greater the rate of free-volume entrapment within the secondary crystalline phase as processing temperature increase up to 190°C. Above 200°C an increase in shear intensity produces a corresponding increase in the amount of occluded free-volume; however, Figure 8 also reveals, unexpectedly, that a process is in operation reducing the free-volume content of the sample at a rate which is independent of shear within the shear regimes of twin-screw extrusion and compression molding. Also it is revealed that at temperatures below 190°C the free-volume population of the sample decreases; in other words, in the absence of other effects the bulk density of the sample should increase, with an increase in process shear intensity. The reverse is expected above 200°C.

We¹⁶ reported earlier that the bulk density and wide-angle X-ray diffraction (WAXD) crystallinity index decrease with an increase in processing temperature passing through a minimum in the region 190–200°C. Additionally, equilibrium acetone uptake for the pressed sample passes through a maximum in the same temperature region. These results are perfectly in line with changes in free-volume content of the sample revealed in the present study. In particular, it is shown here that the marginal increase in density and in WAXD crystallinity index or decrease in acetone sorption capacity of sample prepared above 200°C can be attributed to a decrease of free-volume content of the bulk sample.

The study was conducted at the Institute of Polymer Technology (IPT), Loughborough University, U.K. The

author is grateful to the Institute for providing the facilities. The assistance of the following persons is gratefully acknowledged: Dr. J. M. Hutchinson of Nottingham University, U.K., for helpful suggestions pertaining to the model, Dr. B. Mutagahywa of University of Dar-es-Salaam, Tanzania, for assistance with computer programming, Dr. M. Gilbert of IPT and Dr. D. E. Marshall, Signode Corporation, U.S.A., for very useful suggestions.

REFERENCES

1. K. H. Illers, *Makromol. Chem.*, **127**, 1 (1969).
2. K. H. Illers, *J. Macromol. Sci. Phys.*, **B14**(4), 471 (1977).
3. P. J. Flory, *Principles of Polymer Chemistry*, Cornell University Press, Ithaca, NY, 1953, pp. 563-576.
4. J. A. Juijn, J. H. Gisolf, and W. A. de Jong, *Kolloid. Z. Z. Polym.*, **235**, 1157 (1969).
5. S. Ohta, T. Kajiyama, and M. Takayanagi, *Polym. Eng. Sci.*, **16**, 465 (1976).
6. M. Gilbert and J. C. Vyvoda, *Polymer*, **22**, 1134 (1981).
7. M. Gilbert, *Plast. Rubber Int.*, **10**(3), 16 (1985).
8. H. T. Kau and F. E. Filisko, *Macromolecules*, **12**(3), 479 (1979).
9. E. V. Gouinlock, *J. Polym. Sci. Polym. Phys. Ed.*, **13**, 1533 (1975).
10. R. J. Krzewki and E. A. Collins, *J. Macromol. Sci. Phys.*, **B20**(4), 443 (1981).
11. R. J. Krzewki and E. A. Collins, *J. Macromol. Sci. Phys.*, **B20**(4), 465 (1981).
12. M. L. Kashmiri and R. P. Sheldon, *J. Polym. Sci.*, **B7**, 51 (1969).
13. M. S. Ali and R. P. Sheldon, *J. Appl. Polym. Sci.*, **14**, 2619 (1970).
14. M. S. Ali and R. P. Sheldon, *J. Polym. Sci.*, **C38**, 97 (1972).
15. E. A. Collins, *Pure Appl. Chem.*, **49**, 581 (1977).
16. O. P. Obande and M. Gilbert, *J. Appl. Polym. Sci.*, **37**, 1713 (1989).

Received September 20, 1989

Accepted June 19, 1990